J Mater Sci (2022) 57:444–452

Computation & theory

A theoretical study of gas adsorption on tin arsenic and its application as a highly sensitive NO_2 sensor

Yi Huang[1], Lixiang Wang[1], Qi Wang[1,*], Wensheng Yan[1], Hongsheng Zhang[1], Weizhong Chen[1], and Chengzhang Zhu[2,*]

[1] *School of Optoelectronic Engineering, Chongqing University of Posts and Telecommunications, Chongqing, China*
[2] *School of Environmental and Chemical, Engineering, Jiangsu University of Science and Technology, Zhenjiang, China*

Received: 16 August 2021
Accepted: 9 November 2021
Published online:
3 January 2022

ABSTRACT

The sensing performance of tin arsenic (SnAs) monolayer with adsorption of different gas molecules at room temperature was systematically investigated by the first-principle calculations. The interaction of all studied gas molecules with SnAs monolayer shows physisorption nature. The moderate adsorption energy (− 0.76 eV) and large charge transfer (0.21 e) results demonstrated that the SnAs monolayer is ultra-sensitive to NO_2. And the sensitivity of the SnAs layer for NO_2 detecting is ultra-high reach to 67,500%. Moreover, the SnAs monolayer cannot detect SO_2 and NH_3 gases, which could improve the reliability of the devices, comparing with other two-dimensional (2D) materials that are responsive to NO_2, SO_2, and NH_3 gas molecules. The desorption time of the SnAs device is also short for NO_2 molecules to meet the requirement of reuse. The study demonstrates the potential applications of SnAs in NO_2 detecting with high selectivity and sensitivity at room temperature.

Handling Editor: Yaroslava Yingling.

Address correspondence to E-mail: wangqi@cqupt.edu.cn; zhucz@just.edu.cn

https://doi.org/10.1007/s10853-021-06715-2

GRAPHICAL ABSTRACT

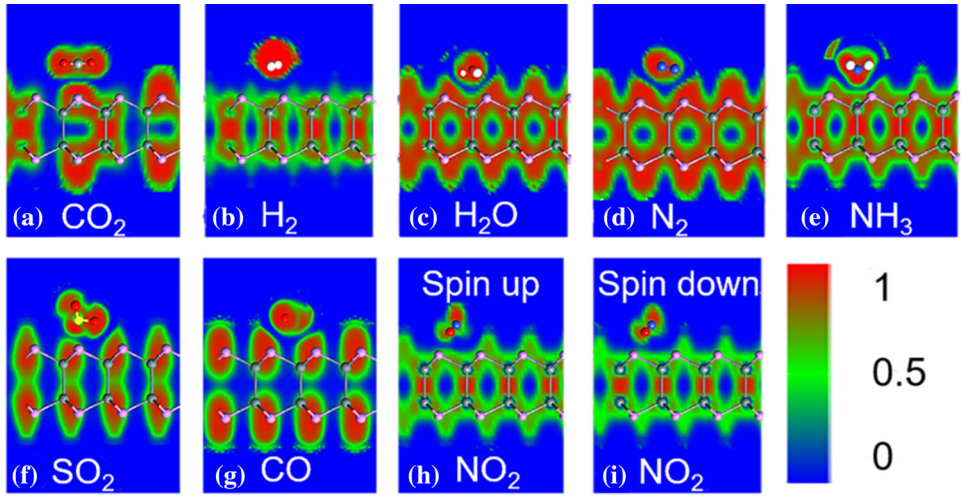

Introduction

Nitrogen dioxide (NO_2), released from human activities and industrial processes such as automobile exhaust and fossil fuel combustion, remains one of the significant air pollutions, which plays a major role in forming ozone and acidifying rain [1–5]. Besides, according to the report of the U.S. EPA, placing oneself in NO_2 concentration over 53 ppb for a long time will seriously harm children's respiratory health and even increase the risk of acute respiratory illness [6]. Therefore, reliable and precise NO_2 gas sensors with high sensitivity and selectivity have been indispensably required for environmental monitoring and public health. However, traditional metallic oxide sensors for NO_2 gas detection require high operating temperatures (> 200 °C). What's worse, these devices also perform poorly at detection limits, often larger than 1 ppm [7–13].

Recently, it has been reported that gas sensors take 2D materials (graphene, MoS_2, black phosphorous, etc.) as sensitive material could detect deleterious gases at room temperature [14–21]. This brings a new dawn for the preparation of high precision and sensitivity room temperature NO_2 gas sensors. However, these materials will still respond to gases other than NO_2 gases, such as SO_2 and NH_3. [22–27]. This could seriously decrease the accuracy of the device and even results in wrong test results. Thus, it is necessary to find more suitable materials as an alternative to detecting NO_2 gases with high selectivity.

SnAs, a new material of IV-V compounds, have been found to have a similar structure to MoS_2 with high carrier mobility and good air-stability [28]. Based on its superior electronic characteristics, we study the sensing performance of several typical molecules on SnAs monolayer to explore their potential applications in NO_2 detecting.

Methods

All atomistic calculations in this work are performed using the density functional theory solved by the Quantum Espresso software. As for exchange–correlation potential, we adopt the common generalized gradient approximation (GGA) in conjunction with Perdew–Burke–Ernzerhof (PBE) functional. The electronic density is described by the Fritz Haber Institute (FHI) pseudopotentials together with double-ζ basis sets [29]. The optimized lattice constants of α-SnAs monolayer are $a = b \approx 4.09$ Å, which is in line with the previous study. The GGA-PBE method usually underestimates the bandgap due to the delocalization and static correlation error [30, 31]. In

this paper, the GGA-1/2 method has been employed for a more accurate bandgap, which corrects the DFT self-interaction error by defining an atomic self-energy potential that cancels the electron–hole self-interaction energy [32]. To give further credit to the calculations, we primarily compared the bandgap of the pristine material with the previous data [28], which confirmed the high reliability of the models and methods. We select a 3 × 3 supercell for adsorption calculation. The *k*-point in the Monkhorst–Pack grid is set to 6 × 10 × 1 for the Brillouin zones sample, and the density mesh cut-off is set to 150 Hartree. The vacuum region along the *z*-axis is set to 15 Å to prevent the interaction between two adjacent slabs.

To explore the interaction property of each adsorption case, we have to obtain the most stable adsorption configurations of SnAs monolayer with adsorption of different gas molecules first. We assume that the initial distance of all the gas molecules from the SnAs surface is a moderate distance of 3 Å. In addition, the influence of different sites on the adsorption model was also considered. Finally, the most stable adsorption configurations are obtained by optimizing the atomic structure of the models until the force tolerance on each atom is less than 0.05 eV/Å.

The adsorption energy is calculated by: $E_a = E_{total} - E_{SnAs} - E_{gas}$, where E_{gas}, E_{SnAs}, and E_{total} are the energy of the gas molecule, SnAs monolayer, and molecule-SnAs systems, respectively. The thermal stability of NO_2-adsorbed SnAs monolayer is calculated by the moles − volume − temperature (NVT) Berendsen ensemble based on molecular dynamics (MD) simulations [33]. The process is carried out under the temperature of 300 K for 3 ps with a time step of 1 fs.

Results and discussion

Before exploring the sensing properties of the adsorption of gas molecules on SnAs monolayer, we first give the most stable adsorption configurations in Fig. 1. In addition, the equilibrium distance (d_0), adsorption energy (E_a), Mulliken charge transfer (Q), and bandgap (E_g) are listed in Table 1.

Figure 1 shows the most stable configurations of different gas molecular adsorption systems. It can be seen that the atomic structure of SnAs monolayer does not undergo obvious deformation or destruction after adsorption of these gas molecules, indicating that there is no chemical reaction between these gas molecules and SnAs. Besides, the d_0 of each gas molecule adsorption systems (Table 1) is obviously longer than the sum of their covalent bond length [34]. Based on these two points, we preliminarily inferred that all gas molecules interact with SnAs monolayer through physical adsorption processes. One thing to note is that the distance between O and As atoms in NO_2-SnAs system is closer to the length of the covalent bond, indicating strong physical adsorption between NO_2 molecules and SnAs monolayer with van der Waals interactions.

The larger adsorption energy of adsorbate adsorbs on gas sensor materials means a higher level of selectivity for detecting [35]. The E_a of NO_2 adsorbed on SnAs monolayer (− 0.76 eV) is obviously higher than that of the others, indicating that SnAs monolayer has a higher selective adsorption capacity for NO_2 than the remaining gas molecules. This means that SnAs-based gas sensors have the potential to detect NO_2 molecules rapidly in complex gas environments.

The sensitivity of the semiconductor film is significantly positively correlated with the amount of charge transfer [14]. To realize the gas sensor only responds to specific gas molecules, it must meet the large charge transfer between the gas-sensitive material and the detected gas molecules. As shown in Table 1, the charge transfer of NO_2 (− 0.210 *e*) molecules adsorbed on SnAs monolayer is surprisingly larger than that of the other gas molecules (all less than 0.04 e). The negative sign of Q in Table 1 means the transfer of charge from SnAs to molecules. This means that when NO_2 molecules are adsorbed on SnAs monolayer, the charges on the surface of SnAs will be exhausted.

Thus, the adsorption of NO_2 molecules can be considered to be similar to the acceptors doping process. The charge transfer results suggest that the electrostatic interactions between NO_2 molecules and SnAs monolayer are stronger than those in the other gas molecules adsorption systems. Therefore, the SnAs monolayer is supposed to be the most sensitive to NO_2 among the calculated gas molecules. It should be pointed out that SnAs monolayer is insensitive to SO_2 and NH_3 molecules. However, MoS_2 and black phosphorous still respond to SO_2, NH_3, etc. [25, 26]. This means a higher selectivity and accuracy of SnAs

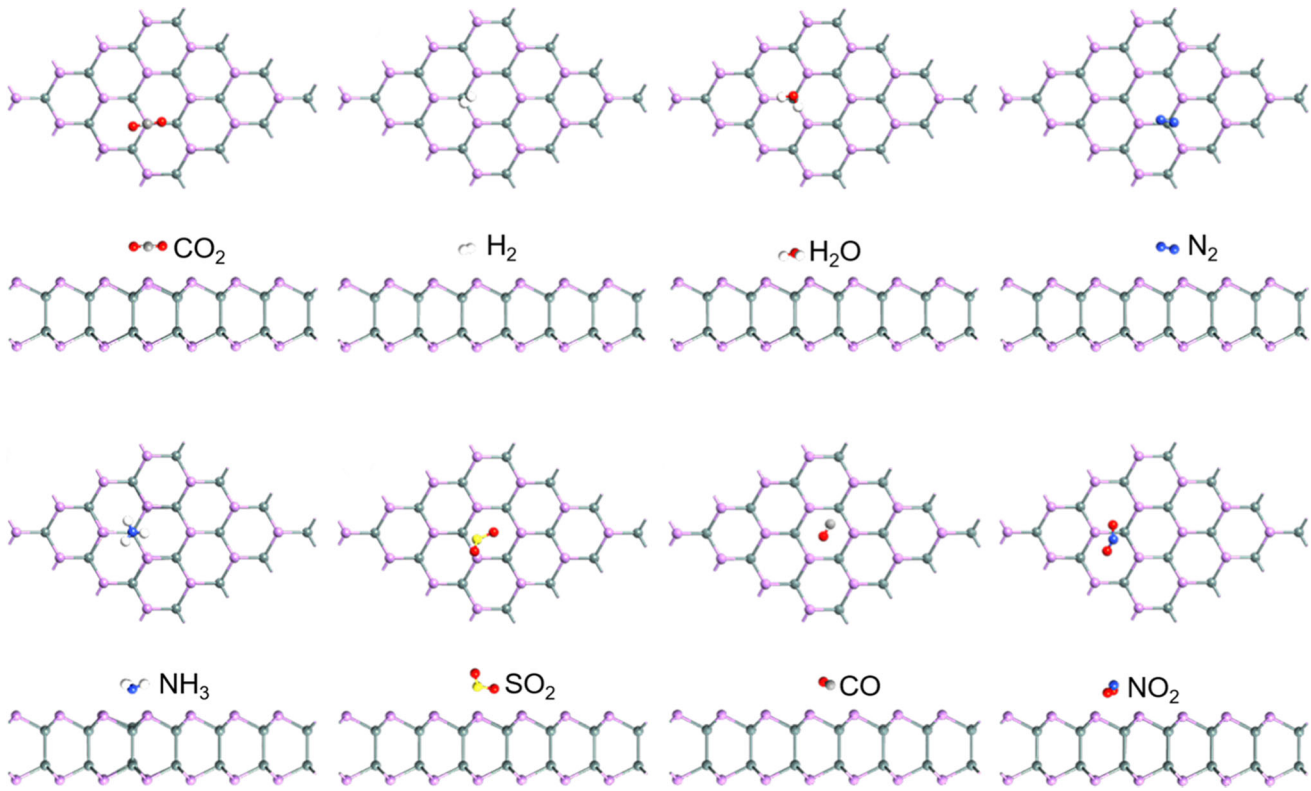

Figure 1 The most stable configurations of different gas molecular adsorption systems: **a** CO_2, **b** H_2, **c** H_2O, **d** N_2, **e** NH_3, **f** SO_2, **g** CO and **h** NO_2.

Table 1 The adsorption properties of different gas adsorption systems

Molecule	E_a(eV)	d_0 (Å)	Q (e)	E_g(direct)
CO_2	− 0.29	3.08 (As-C)	0.001	1.35
H_2	− 0.15	3.36 (As-H)	− 0.012	1.35
H_2O	− 0.53	2.71 (As-H)	0.001	1.35
N_2	− 0.40	3.38 (As-N)	0.03	1.35
NH_3	− 0.46	3.25 (As-N)	0.04	1.35
SO_2	− 0.57	2.92 (As-S)	0.001	1.05
CO	− 0.44	3.19 (As-C)	− 0.023	1.33
NO_2	− 0.76	2.69 (As-O)	− 0.210	Spin up/down 1.27/0.38

materials for NO_2 detecting than that with black phosphorus and MoS_2 because the latter two materials are also responsive to SO_2 [36].

In addition, the adsorption of NO_2 molecules will significantly change the electron band structure of SnAs monolayer. The bandgap of SnAs monolayer decreased rapidly from the direct bandgap of 1.12 eV to the indirect bandgap of 0.34 eV. However, the adsorption of other gas molecules only slightly disturbs their electronic structure, and the bandgap changes are not noticeable.

After adsorption of the gas molecules, the charge distribution of material will be disturbed and then redistribute to the most stable state. The electron localization function (ELF) of different gas adsorbed systems is presented in Fig. 2. It can be seen that the electron localization of SnAs monolayer did not overlap with any calculated gas molecules, indicating that the process of these adsorbates adsorb on the surface of SnAs monolayer is the physisorption nature. This result is consistent with preliminary judgment by the equilibrium distance in Table 1.

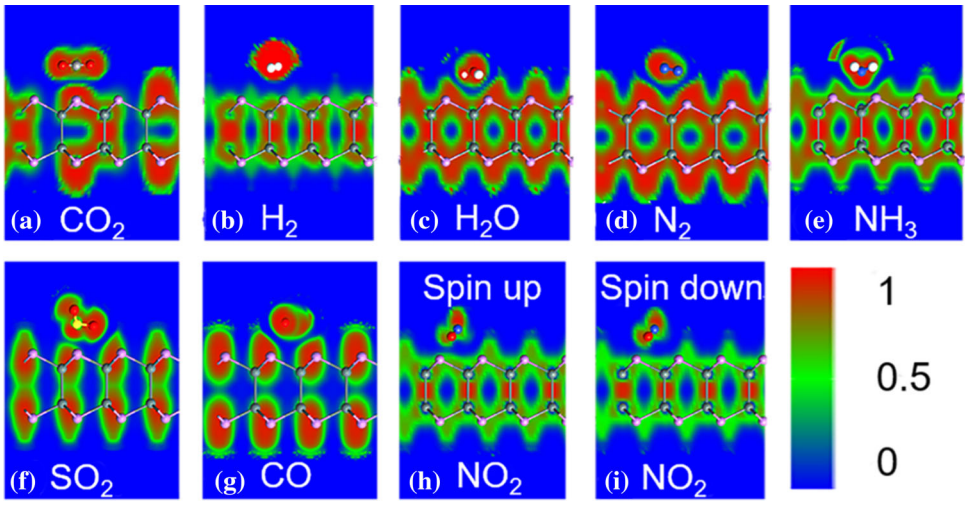

Figure 2 The ELF calculations of different gas molecular adsorption systems: **a** CO_2, **b** H_2, **c** H_2O, **d** N_2, **e** NH_3, **f** SO_2, **g** CO, **h** NO_2 spin up and **i** NO_2 spin down.

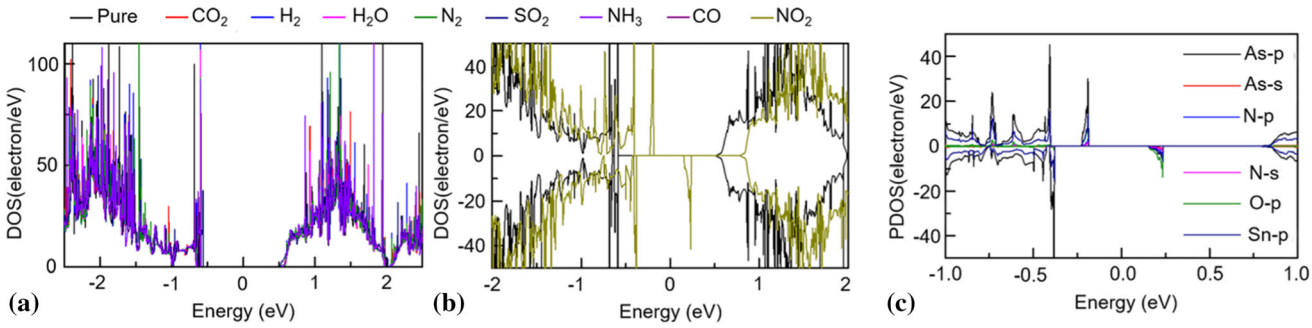

Figure 3 The DOS of pure SnAs and **a** CO_2, H_2, H_2O, N_2, SO_2, NH_3 and CO, and **b** NO_2 molecules adsorbed on the SnAs. **c** The PDOS of NO_2 -SnAs adsorption system. **d** Total energy fluctuations with time for NO_2-adsorbed SnAs monolayer at T = 300 K with molecular dynamics simulation. Inset: structural configurations after 1 ps, 2 ps, and 3 ps.

To further understand the inherent charge transfer characteristics of the SnAs monolayer after adsorption of gas molecules, the electronic density of states (DOS) of each adsorption case is present in Fig. 3a and b. We can find that the DOS close to the Fermi level has not altered much with the adsorption of other seven gas molecules except NO_2 molecule, indicating that these molecules do not change the electronic characteristics of SnAs monolayer visibly. These results are consistent with previous charge transfer values.

The curve of DOS shifts to the right by about 0.25 eV after the NO_2 molecule adsorption and new electronic states are formed around ± 0.20 eV, as plotted in Fig. 3c. These newly formed electronic states have dual effects on the carrier capture and transportation, which could alter the electronic characteristics of the SnAs monolayer. We present the atom projected density of states (PDOS) of the NO_2-SnAs system in Fig. 3c to figure out where these electronic states are coming from. The main contribution of orbital hybridization comes from the p orbitals of As, Sn atoms from SnAs monolayer and the p orbitals of N and O atoms from NO_2 molecule within the range − 0.226 to − 0.185 eV and 0.151 to 0.238 eV. Therefore, it can be concluded that the superior charge transfer can be attributed to the hybridization behavior in p orbital of atoms between the adsorbate and SnAs monolayer .

The MD result shows that the energy of the NO_2 adsorbed system rises significantly within the initial 0.5 ps and then fluctuates around a certain constant, implying that the simulation has reached the equilibrium state and the structure of the NO_2 adsorbed system will not collapse due to thermal fluctuation, as shown in Fig. 4a. There is no obvious structural distortion or transformation that occurs in the system during the whole process, as presented in Fig. 4b. Put it in another way, the structural stability was not changed with the NO_2 adsorbed. Our results show

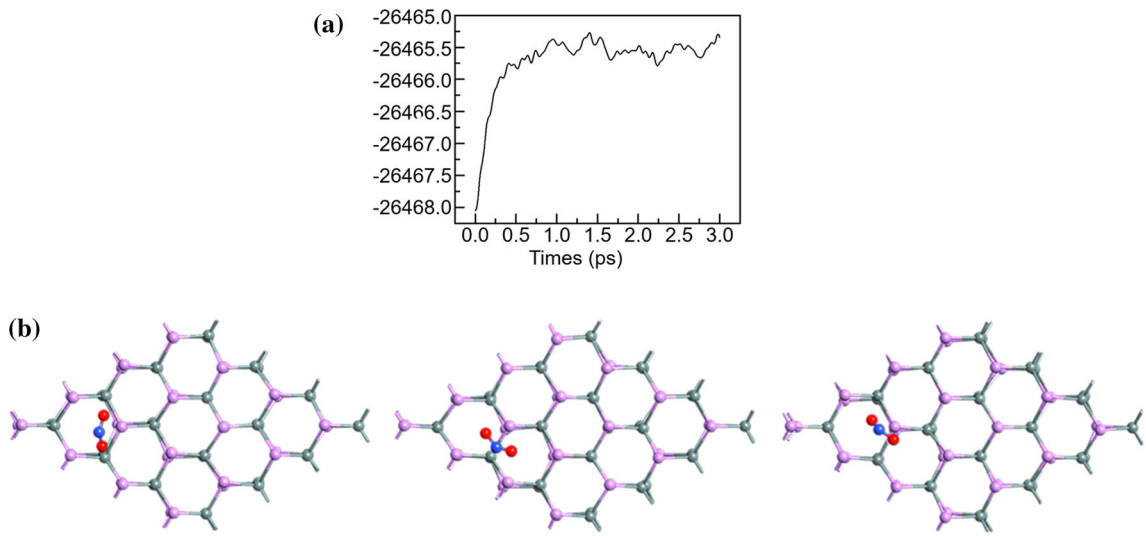

Figure 4 **a** Total energy fluctuations with time for NO_2-adsorbed SnAs monolayer at T = 300 K with molecular dynamics simulation. **b** Structural configurations after 1 ps, 2 ps, and 3 ps.

that SnAs monolayer is thermodynamically stable with adsorption of NO_2 molecules at room temperature. Hence, one can expect that the SnAs monolayer can be realized for NO_2 detecting in practice.

Sensitivity is a critical index of the sensor performance, which is defined as follows: $S = \frac{\sigma - \sigma_0}{\sigma_0} \times 100\%$, where σ_0 and σ are the electrical conductivity of the gas sensor before and after gas adsorption, respectively. The electrical conductivity related to the bandgap is expressed as: $\sigma = AT^{3/2}\exp(\frac{-E_g}{2k_BT})$ [37–42], where A is the system-dependent constant of proportionality (electrons m^{-3} $K^{-3/2}$), k_B is the Boltzmann constant, T is the temperature (K), and E_g is the energy bandgap of the system. An average spin gap was calculated from the two spin conserving gaps. The sensitivity of the SnAs layer for NO_2 detecting is ultra-high reach to 67,500%. This magnitude indicates that the SnAs layer is ultra-sensitive to NO_2.

The recovery time of the NO_2 gas molecules desorption from SnAs monolayer at room temperature is estimated to be 5.85 s by using the transmission state theory through the formula: $\tau = v_0^{-1}e^{(-E_a/kT)}$, where v_0 is the attempt frequency of NO_2 with the value of 10^{12} s^{-1}, and k is the Boltzmann constant [43, 44]. The result further indicates that the SnAs monolayer is an excellent gas-sensitive material for NO_2 detection and can be reused (Table 2).

In recent years, a huge family of 2D materials has been predicted for NO_2 detecting. Furthermore, we compared the adsorption energy and the electron charge transfer with previous researches. It can be found that SnAs monolayer has moderate adsorption energy and large charge transfer with the NO_2 adsorption, comparing with graphene, arsenene, MoS_2, and phosphorene. It should be noted that the charge transfer for NO_2 adsorbing on the silicene and antimonene monolayer is much larger than SnAs. This is because that the NO_2 molecular adsorbed on the silicene and antimonene monolayer is chemisorption process. The desorption of gas from the surface would be very hard due to the strong chemical adsorption of gas molecules on these materials, which is not suitable for reuse.

In conclusion, the sensitivity (67,500%) of the SnAs layer for NO_2 detecting demonstrates the SnAs monolayer is ultra-selective to NO_2 molecule among all investigated gas molecules. Moreover, SnAs is insensitive to other reactive gas molecules like SO_2 and NH_3, which benefits the detection reliability, comparing with graphene and black phosphorus. In addition, our results show that the SnAs-based gas sensor is thermodynamically stable at room temperature after NO_2 adsorption and performs a short recovery time of 5.85 s. Therefore, SnAs could be considered to be one of the best candidate materials for NO_2 detection with ultra-selective at room temperature.

Table 2 The theoretically reviewed 2D materials for NO_2 detecting, the corresponding adsorption energy and the amount of charge transfer to the layered materials are listed

Materials	Adsorption energy (eV)	Amount of charge transfer (e)	Remarks	Reference
Graphene	0.055–0.067	0.1	Physisorption, no vdW correction	[45]
Silicene	1.30	0.37	Chemisorption	[46]
Arsenene	0.44	0.187		[47]
Antimonene	0.813	0.337	NO_2 chemiadsorbed	[48]
MoS_2	0.28	–	Binding energies are corrected with optPBE-vdW	[49]
Phosphorene	0.62	0.2		[50]
SnAs	0.76	0.21		This work

Acknowledgements

This work was supported by the technology Innovation and Application Demonstration key Project of Chongqing Municipality [cstc2019jszx-zdztzxX0005], the technology Innovation and Application Demonstration key Project of Chongqing Municipality [cstc2020jscx-gksbX0011], Chongqing Basic and Frontier Research Project (cstc2018jcyjAX0209).

References

[1] Cleemput OV, Samater AH (1995) Nitrite in soils: accumulation and role in the formation of gaseous N compounds. Fertil Res 45:81–89

[2] Canales M, Marcos A, Zárate A, Magaña LF (2020) Effects of masking titanium with a one-atom-thick carbon layer on the adsorption of nitrogen monoxide, nitrogen dioxide, ozone, and formaldehyde. J Mater Sci 55:17000–17018. https://doi.org/10.1007/s10853-020-05238-6

[3] Wu X, Guan R, Zheng W-T, Huang K, Liu F (2021) Developing porous organic polymers as precursors of nitrogen-decorated micro-mesoporous carbons for efficient capture and conversion of carbon dioxide. J Mater Sci 56:9315–9329. https://doi.org/10.1007/s10853-021-05835-z

[4] Camargo JA, Alonso A (2006) Ecological and toxicological effects of inorganic nitrogen pollution in aquatic ecosystems: a global assessment. Environ Int 32:831–849. https://doi.org/10.1016/j.envint.2006.05.002

[5] Guarnieri M, Balmes JR (2014) Outdoor air pollution and asthma. Lancet 383:1581–1592. https://doi.org/10.1016/s0140-6736(14)60617-6

[6] Lamsal LN, Duncan BN, Yoshida Y et al (2015) U.S. NO2 trends (2005–2013): EPA air quality system (AQS) data versus improved observations from the ozone monitoring instrument (OMI). Atmos Environ 110:130–143. https://doi.org/10.1016/j.atmosenv.2015.03.055

[7] Dong X, Wu K, Zhu W et al (2019) TiO2 nanotubes/g-C3N4 quantum dots/rGO Schottky heterojunction nanocomposites as sensors for ppb-level detection of NO2. J Mater Sci 54:7834–7849. https://doi.org/10.1007/s10853-019-03468-x

[8] Geeta Rani B, Saisri R, Kailasa S, Sai Bhargava Reddy M, Maseed H, Venkateswara Rao K (2020) Architectural tailoring of orthorhombic MoO3 nanostructures toward efficient NO2 gas sensing. J Mater Sci 55:8109–8122. https://doi.org/10.1007/s10853-020-04601-x

[9] Zheng X, Zhang C, Xia J et al (2018) Sensing properties of amperometric ppb-level NO2 sensor based on sodium ion conductor with sensing electrodes comprising different WO3 nanostructures. J Mater Sci 54:5311–5320. https://doi.org/10.1007/s10853-018-03189-7

[10] Eranna G, Joshi BC, Runthala DP, Gupta RP (2010) Oxide materials for development of integrated gas sensors—a comprehensive review, Crit Rev. Solid State & Mater Sci 29:111–188. https://doi.org/10.1080/10408430490888977

[11] Fine GF, Cavanagh LM, Afonja A, Binions R (2010) Metal oxide semi-conductor gas sensors in environmental monitoring. Sensors (Basel) 10:5469–5502. https://doi.org/10.3390/s100605469

[12] Lu B, Liu R, Li S, Lu R, Chen L, Ye Z, Lu J (2020) Room-temperature processed amorphous ZnRhCuO thin films with p-Type transistor and gas-sensor behaviors. Chinese Phys Lett 37:098501. https://doi.org/10.1088/0256-307x/37/9/098501

[13] Panahi N, Hosseinnejad MT, Shirazi M, Ghoranneviss M (2016) Optimization of gas sensing performance of nanocrystalline SnO2 thin films synthesized by magnetron sputtering. Chinese Phys Lett 20:066802. https://doi.org/10.1088/0256-307x/33/6/066802

[14] Cui S, Pu H, Wells SA, Wen Z, Mao S, Chang J, Hersam MC, Chen J (2015) Ultrahigh sensitivity and layer-

dependent sensing performance of phosphorene-based gas sensors. Nat Commun 6:8632. https://doi.org/10.1038/ncomms9632

[15] Mathew M, Shinde PV, Samal R, Rout CS (2021) A review on mechanisms and recent developments in p-n heterojunctions of 2D materials for gas sensing applications. J Mater Sci 56:9575–9604. https://doi.org/10.1007/s10853-021-05884-4

[16] Harale NS, Dalavi DS, Mali SS, Tarwal NL, Vanalakar SA, Rao VK, Hong CK, Kim JH, Patil PS (2018) Single-step hydrothermally grown nanosheet-assembled tungsten oxide thin films for sensitive and selective NO2 gas detection. J Mater Sci 53:6094–6105. https://doi.org/10.1007/s10853-017-1905-9

[17] Jiang T, He Q, Bi M, Chen X, Sun H, Tao L (2021) First-principles calculations of adsorption sensitivity of Au-doped MoS2 gas sensor to main characteristic gases in oil. J Mater Sci 56:13673–13683. https://doi.org/10.1007/s10853-021-06168-7

[18] Kumar R, Goel N, Kumar M (2017) UV-activated MoS2 based fast and reversible NO2 sensor at room temperature. ACS Sens 2:1744–1752. https://doi.org/10.1021/acssensors.7b00731

[19] Sun D, Luo Y, Debliquy M, Zhang C (2018) Graphene-enhanced metal oxide gas sensors at room temperature: a review. Beilstein J Nanotechnol 9:2832–2844. https://doi.org/10.3762/bjnano.9.264

[20] Ghadiri M, Ghashghaee M, Ghambarian M (2020) Influence of NiO decoration on adsorption capabilities of black phosphorus monolayer toward nitrogen dioxide: periodic DFT calculations. Mol Simulat 46(14):1062–1072. https://doi.org/10.1080/08927022.2020.1802023

[21] Ghashghaee M, Ghambarian M (2020) Defect engineering and zinc oxide doping of black phosphorene for nitrogen dioxide capture and detection: quantum-chemical calculations. Appl Surf Sci 523:146527. https://doi.org/10.1016/j.apsusc.2020.146527

[22] Yang Q, Meng RS, Jiang JK, Liang QH, Tan CJ, Cai M, Sun X et al (2016) First-principles study of sulfur dioxide sensor based on phosphorenes. IEEE Electr Device L 37:660–662. https://doi.org/10.1109/led.2016.2543243

[23] Abudukeremu H, Kari N, Zhang Y, Wang J, Nizamidin P, Abliz S, Yimit A (2018) Highly sensitive free-base-porphyrin-based thin-film optical waveguide sensor for detection of low concentration NO2 gas at ambient temperature. J Mater Sci 53:10822–10834. https://doi.org/10.1007/s10853-018-2374-5

[24] Singh I, Bedi RK (2011) Influence of pH on the synthesis and characterization of CuO powder for thick film room-temperature NH3 gas sensor. J Mater Sci 46:5568–5580. https://doi.org/10.1007/s10853-011-5507-7

[25] Zhao MY, Zhang DY, Dong S (2021) DFT study of NO2 and SO2 gas-sensing properties of InX (X = Cl, Br and I) monolayers. J Mater Sci 56:11828–11837. https://doi.org/10.1007/s10853-021-06047-1

[26] Nithya S, Dutta A (2021) Electrochemical sensing of trace level NH3: active electrode and electrolyte optimizations. J Mater Sci 56:6269–6285. https://doi.org/10.1007/s10853-020-05654-8

[27] Jia A, Liu B, Liu H, Li Q, Yun Y (2020) Interface design of SnO2@PANI nanotube with enhanced sensing performance for ammonia detection at room temperature. Front Chem 8:383. https://doi.org/10.3389/fchem.2020.00383

[28] Zhou D, Zheng Y, Pu C, Wang Z, Tang X (2018) Computational prediction to two-dimensional SnAs. Chinese Phys Lett 35:107101. https://doi.org/10.1088/0256-307x/35/10/107101

[29] Blum V, Gehrke R, Hanke F, Hanke F, Havu P, Havu V, Ren X, Reuter K, Scheffler M (2009) Ab initio molecular simulations with numeric atom-centered orbitals. Comput Phys Commun 180:2175–2196

[30] Cohen AJ, Mori-Sánchez P, Yang W (2008) Insights into current limitations of density functional theory. Science 321:792–794. https://doi.org/10.1126/science.1158722

[31] Mori-Sánchez P, Cohen AJ, Yang W (2008) Localization and delocalization errors in density functional theory and implications for band-gap prediction. Phys Rev Lett 100:146401. https://doi.org/10.1103/PhysRevLett.100.146401

[32] Ferreira LG, Marques M, Teles LK (2008) Approximation to density functional theory for the calculation of band gaps of semiconductors. Phys Rev B 78:125116. https://doi.org/10.1103/PhysRevB.78.125116

[33] Berendsen HJC, Postma JPM, van Gunsteren WF, DiNola A, Haak JR (1984) Molecular dynamics with coupling to an external bath. J Chem Phys 81:3684–3690. https://doi.org/10.1063/1.448118

[34] Pyykko P, Atsumi M (2009) Molecular single-bond covalent radii for elements 1–118. Chemistry 15:186–197. https://doi.org/10.1002/chem.200800987

[35] Wang J, Lei JM, Yang GF, Xue JJ, Cai Q, Chen DJ, Lu H, Zhang R, Zheng YD (2018) An ultra-sensitive and selective nitrogen dioxide sensor based on a novel P2C2 monolayer from a theoretical perspective. Nanoscale 10:21936–21943. https://doi.org/10.1039/c8nr05568h

[36] Chen D, Zhang X, Tang J, Cui H, Li Y (2018) Noble metal (Pt or Au)-doped monolayer MoS2 as a promising adsorbent and gas-sensing material to SO2, SOF2 and SO2F2: a DFT study. Appl Phys A. https://doi.org/10.1007/s00339-018-1629-y

[37] Ghadiri M, Ghambarian M, Ghashghaee M (2020) Detection of CNX cyanogen halides (X = F, Cl) on metal-free defective phosphorene sensor: periodic DFT calculations. Mol Phys. https://doi.org/10.1080/00268976.2020.1819577

[38] Ghambarian M, Azizi Z, Ghashghaee M (2018) Remarkable improvement in phosgene detection with defectengineered phosphorene sensor: first-principles calculations. Phys Chem Chem Phys. https://doi.org/10.1039/D0CP00427H

[39] Marjani A, Ghambarian M, Ghashghaee M (2021) Alkali metal doping of black phosphorus monolayer for ultrasensitive capture and detection of nitrogen dioxide. Sci Rep. https://doi.org/10.1038/s41598-020-80343-9

[40] SO Kasap (2018) Principles of electronic materials and devices. 4th edn

[41] BS Mitchell (2004) An introduction to materials engineering and science. 4th edn

[42] C Kittel (2005) Introduction to solid state physics. 8th edn

[43] Peng S, Cho K, Qi P, Dai H (2004) Ab initio study of CNT NO2 gas sensor. Chem Phys Lett 387:271

[44] Zhu C, Xian Q, He Q et al (2021) Edge-Rich bicrystalline 1T/2H-MoS2 cocatalyst-decorated 110 terminated CeO2 nanorods for photocatalytic hydrogen evolution. ACS Appl Mater Interfaces 13:35818. https://doi.org/10.1021/acsami.1c09651

[45] Leenaerts O, Partoens B, Peeters F (2008) Adsorption of H2O, NH3, CO, NO2, and NO on graphene: a first-principles study. Phys Rev B 77:1254146. https://doi.org/10.1103/PhysRevB.77.125416

[46] Prasongkit J, Amorim R, Chakraborty S, Ahuja R, Scheicher R, Amornkitbamrung V (2015) Highly sensitive and selective gas detection based on silicene. J Phys Chem C 119:16934–16940

[47] Chen X, Wang L, Sun X, Meng RS, Xiao J, Ye HY, Zhang GQ (2017) Sulfur dioxide and nitrogen dioxide gas sensor based on arsenene: a first-principle study. IEEE Electr Device L 38:661–664

[48] Meng RS, Cai M, Jiang JK, Liang QH, Sun X, Yang Q (2017) First principles investigation of small molecules adsorption on antimonene. IEEE Electr Device L 38:134–137

[49] Zhao S, Xue J, Kang W (2014) Gas adsorption on MoS2 monolayer from first-principles calculations. Chem Phys Lett 595:35–42

[50] Kou L, Frauenheim T, Chen C (2014) Phosphorene as a superior gas sensor: Selective adsorption and distinct I-V response. J Phy Chem Let 5:2675–2681